

# Ice Adhesion on Superhydrophobic and Hydrophobic Surfaces: Effect of Wetting Hysteresis

S.A. Kulinich, M. Farzaneh, and S. Farhadi

NSERC / Hydro-Quebec / UQAC Industrial Chair on Atmospheric Icing of Power Network Equipment (CIGELE) and  
 Canada Research Chair on Engineering of Power Network Atmospheric Icing (INGIVRE) <http://cigele.ca>  
 at Université du Québec à Chicoutimi, Chicoutimi, QC, Canada

**Abstract—** In this work, ice adhesion strength on flat hydrophobic and rough superhydrophobic coatings with similar surface chemistry (all based on same fluoropolymer) is compared. Artificially created glaze ice, similar to naturally accreted ice, was accreted on the surfaces by spraying super-cooled water microdroplets in a wind tunnel at subzero temperature. Ice adhesion strength was evaluated by spinning the samples in a centrifuge at constantly increasing rotational speed until ice delamination occurred. Bare polished aluminum, flat hydrophobic and rough superhydrophobic surfaces with different contact angle hysteresis were tested, clearly showing that the latter, along with the contact angle, also influences the ice-solid adhesion strength.

**Keywords:** Superhydrophobicity; Roughness; Water contact angle; Wetting hysteresis; Ice adhesion; Shear stress

## I. INTRODUCTION

Ice and wet-snow adhesion to outdoor surfaces is known to cause serious problems to power transmission lines, aircrafts, boats, etc. [1-3]. Even though there is no known material that completely prevents ice/snow build-ups on its surface [2-4], some coatings are believed to provide reduced adhesion. This is expected to result in lower ice and/or wet-snow accumulation on such coated surfaces. Therefore, the research on coatings capable of reducing frost, wet-snow and/or ice accumulation has been going on for decades [1-14]. Good correlation between hydrophobicity of surfaces and their ice-repellent behaviour was previously reported by several groups [11,14]. It was, however, argued down by others [15], who found no correlation between the ice adhesion data and the contact angle (CA) on plastic surfaces. Superhydrophobic surfaces (i.e. those exhibiting water CA > 150°) were tested by Saito *et al.*, and demonstrated promising anti-icing performance [11]. However, no systematic work on ice-repellent superhydrophobic surfaces has been reported since then.

Several methods have been proposed to evaluate ice-solid adhesion [2,4,5,8,10,11,14-16]. In most cases, however, water had been artificially frozen on top of the samples tested under unrealistic icing conditions [2,8,11,14,16]. Therefore, testing adhesion of glaze ice prepared by spraying super-cooled water droplets is expected to give more reliable results [9,10]. In this study, glaze ice was prepared by spraying water microdroplets at subzero temperature, i.e. at conditions very close to outdoor ice accretion. Ice adhesion

was tested on polished aluminium, flat hydrophobic and rough superhydrophobic fluoropolymer surfaces. Superhydrophobic samples with different contact angle hysteresis (CAH) were tested, clearly showing that the latter, along with the CA, also governs the ice-solid adhesion strength.

## II. EXPERIMENT

The coatings were prepared by following and modifying recipes previously reported elsewhere [17,18]. AA6061 aluminium alloy plates, 3.2 x 5.0 cm<sup>2</sup> in size, were used as substrates. Prior to coating, they were polished with emery paper and cleaned in organic solvents. ZrO<sub>2</sub>, AlCeO<sub>3</sub> or CeO<sub>2</sub> nanopowders from Aldrich, 8.0 g in each case, were mixed with 80 ml of deionized water. The suspensions were sonicated for 30 min, after which 5.0 ml of Zonyl 8740 (a perfluoroalkyl methacrylic copolymer product from DuPont) were added. The final suspensions were stirred for 3 h before being coated on the substrates. Superhydrophobic sample 3 was prepared by spraying the ZrO<sub>2</sub> suspension over the substrate surface uniformly and letting it dry at ~50 °C. Superhydrophobic samples 4-6 were prepared by spin-coating corresponding suspensions on the substrate. The particles used and their size are shown in Table 1. Use of different nanoparticles and spray or spin-coating allowed to prepare samples with different surface topographies and wetting hysteresis, as discussed below. Upon coating, the samples were heat-treated at 120 °C in air for 3 h to remove residual solvents. Hydrophobic sample 2 was prepared similarly to sample 3 except that no nanoparticles were added, leading to a flat fluoropolymer surface. Sample 1 was a bare plate of polished Al used as the standard (see Table 1).

Table 1. Hydrophobic properties of the samples analyzed

Sample #	Nanoparticles used	CA (°)	CAH (°)
1	-	57.3 ± 2.8	~50
2	-	120.1 ± 2.3	~40
3	ZrO <sub>2</sub> / 20-30 nm	151.1 ± 2.4	> 70
4	ZrO <sub>2</sub> / 20-30 nm	152.2 ± 1.5	7.7 ± 2.0
5	AlCeO <sub>3</sub> / < 25 nm	153.1 ± 1.4	8.0 ± 2.1
6	CeO <sub>2</sub> / 10-20 nm	151.7 ± 1.6	9.2 ± 2.3

Both CA and CAH values were measured on a Krüss DSA100 contact-angle goniometer following standard procedures. The measurements were made at  $23\pm 0.5$  °C, with 5- $\mu$ L water droplets. Surface topographies were analyzed with a WYKO NT1100 optical profiler (Veeco) and scanning electron microscopy (SEM), JSM 6330-F from JEOL. X-ray photoelectron spectroscopy (XPS) was performed with a Quantum-2000 instrument from ULVAC-PHI.

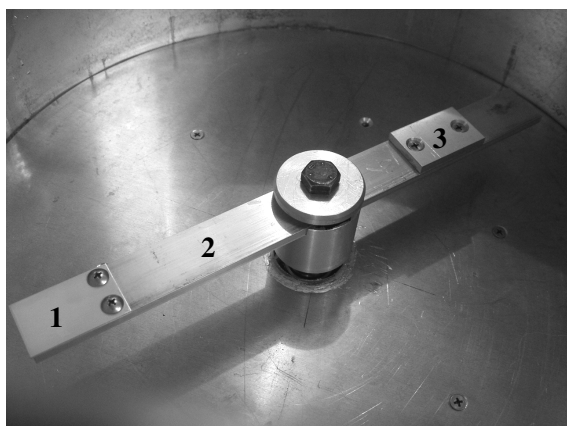


Fig. 1. Coated sample in centrifuge set-up for measuring ice adhesion. (1) Sample, (2) aluminium beam, (3) counter-weight.

The ice adhesion evaluation tests were conducted on Al beams with samples spun in a home-made centrifuge apparatus (see Fig.1). The samples attached to the beams were iced in a wind tunnel at a wind speed of 10 m/s, temperature -10 °C, water feed rate of 2.5 g/m<sup>3</sup> and average droplet size of ~80  $\mu$ m, resulting in glaze ice layers up to ~1 cm thick over the sample area of ~3.2 x 3.0 cm<sup>2</sup>. This ice geometry was enough to avoid cohesion failure and provide well reproducible results during deicing. Ice mass and area were carefully evaluated both before and after deicing. To balance the beam in the centrifuge, a counter-weight was used on the other side (Fig.1). The artificially iced samples were spun in the centrifuge placed in a climatic chamber at -10°C in order to determine the rotational speed at which ice detachment from the sample surface occurred. At the time of the detachment (detected with sensors embedded into the centrifuge walls), the adhesion strength of ice is assumed to be equal to the centrifugal force,  $F = mr\omega^2$ , where  $m$  is the ice mass,  $r$  is the beam radius and  $\omega$  is the rotational speed in rad/s. The shear stress, correspondingly, was calculated as  $\tau = F/A$ , where  $A$  is the deiced area. To reduce the influence of any experimental errors, the adhesion reduction factor,  $ARF$ , was finally used rather than absolute values of shear stress.  $ARF$  was calculated as the ratio of shear stress of ice detachment on sample 1 (bare Al) to that on samples with coatings,  $ARF = \tau_{(Al)}/\tau_{(coating)}$ , provided that all the tests (for both uncoated and coated samples) were run under identical conditions. Three pieces were prepared for each sample in Table 1, and the results were calculated as the average of the three. More details on the ice evaluation technique can be found elsewhere [9,10].

### III. RESULTS AND DISCUSSION

Table 1 compares wetting characteristics of the samples used in this study, and both CA and CAH values are presented. Samples 1 and 2, which are bare polished Al and fluoropolymer-coated Al plates, show CA of ~57 and ~120° and CAH of ~50 and ~40°, respectively. These values are typical for flat hydrophilic and hydrophobic surfaces, respectively. Meanwhile, samples 3-6 prepared with ZrO<sub>2</sub> (3,4), AlCeO<sub>3</sub> (5) or CeO<sub>2</sub> (6) nanoparticles show high values of CA > 150° characteristic of superhydrophobic surfaces.

Only F, Zr (or Ce), C, O and Al peaks were observed in the XPS survey spectra of all superhydrophobic samples 3-6. The presence of the Al signal implies some porosity of the coatings, which is in agreement with their surface images (see e.g. Fig.2). Samples 3 and 4 had very similar composition, as calculated from their XPS spectra. This, taking into account the high values of CA observed for samples 3-6 (see Table 1), implies that all nanoparticles were well covered with fluoropolymer, and thus that all the samples had very similar surface chemistry.

Surface images of rough superhydrophobic samples 3 and 4 are presented in Figs.2 and 3. These figures compare samples 3 (a) and 4 (b) prepared from the same ZrO<sub>2</sub> suspension by means of spraying (Figs.2a,3a) or spin-coating (Figs.2b,3b). Both surfaces are seen to be rough at micro scale, with average roughness ( $R_a$ ) of 192 and 229 nm for samples 3 and 4, respectively. Thus air entrapment into their structure is expected during wetting. However, the surface asperities in Figs.2a,3a are shorter, farther apart and have relatively flat and shallow tops, whereas those in Figs.2b,3b are taller, with sharper appearance and more properly spaced. Therefore, while the Cassie-Baxter wetting mode is expected for sample 4, a mixed (Cassie-Baxter and Wenzel) mode is likely for sample 3 [18]. As a result, the water-solid contact area on sample 3 is expected to be larger than that on sample 4, which is in agreement with the contrasting wetting hysteresis observed on these samples (see insets in Figs.2a and 2b).

Surface images of samples 5 and 6 prepared from AlCeO<sub>3</sub> (5) or CeO<sub>2</sub> (6) nanoparticles were qualitatively similar to those of sample 4 (Figs.2b,3b). In both cases, rough surfaces were observed, implying air entrapment into the structures when water droplet was placed atop. As surface asperities were well separated on both surfaces, high CA and “slippy” surface state were observed on both samples, which is consistent with the low CAH values in Table 1.

As in nature icing events occur under more dynamic conditions than those previously applied for testing ice adhesion on materials [2,8,11,14,16], which implies that the dynamic hydrophobicity of surfaces may play some role. This assumption is in agreement with several previous reports where various dynamic aspects of surface hydrophobicity (in addition to CA) were proposed to be taken into account to characterize surface water repellency [6,12,19-21]. Therefore, to test the influence of the dynamic hydrophobicity of the surface (defined by CAH values) on its icing/deicing behaviour, rough samples with contrasting wetting hysteresis were prepared

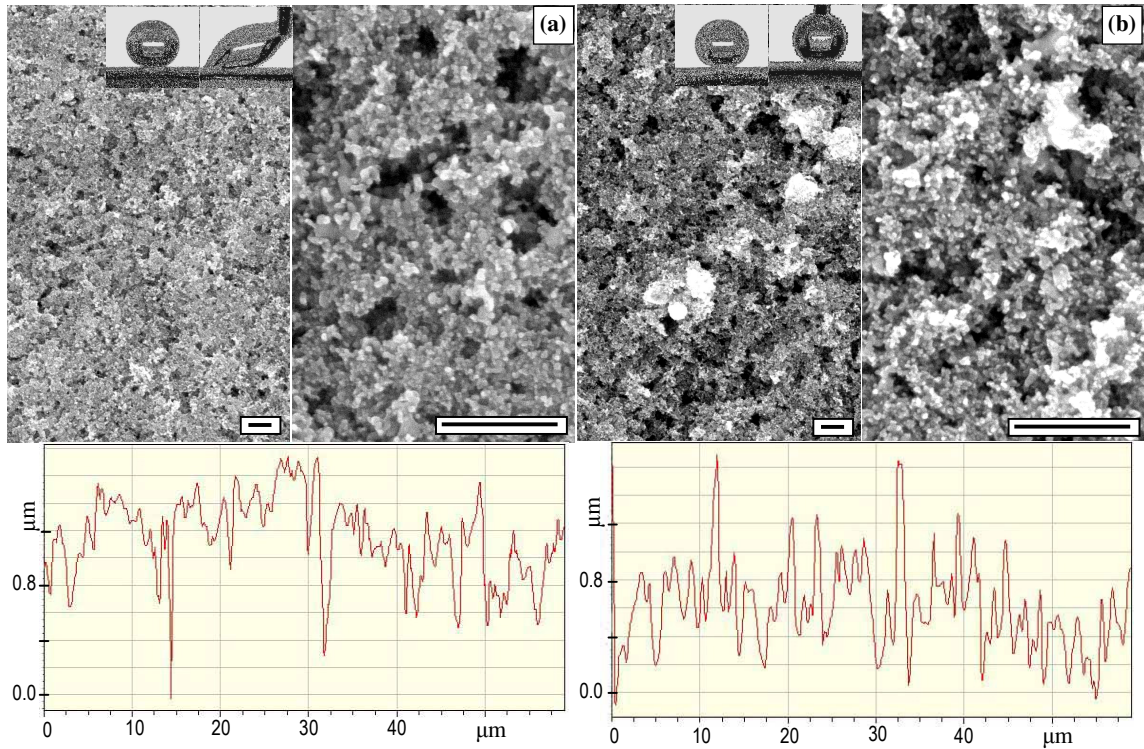


Fig. 2. Surface images and profiles of samples 3 (a) and 4 (b) prepared from  $ZrO_2$  nanopowder. Sessile and moving water droplets are shown as insets. Scale bars indicate 500 nm.

(compare sample 3 with samples 4-6 in Table 1).

Figure 4 presents  $ARF$  values (light-grey columns) obtained for all the samples in Table 1, for convenience,  $CAH$  values are also shown (dark-grey columns). The results obtained on bare Al and flat fluoropolymer-coated samples (1

and 2 in Fig.4) are consistent with those of Somlo and Gupta [8], who reported  $\sim 1.4$ - $2.1$  times lower ice adhesion on organosilane-coated AA6061 when compared to bare AA6061 with various surface finish. It is seen that ice adhesion on the flat fluoropolymer sample 2 is  $\sim 2.5$  times lower than that on the bare polished aluminium (sample 1). This is also in agreement with the general belief that low-energy surfaces demonstrate reduced ice adhesion [2,6,11,12,14].

The  $ARF$  of the high-hysteresis sample 3 is significantly lower when compared to the other superhydrophobic samples, and quite close to that of the uncoated sample 1. Samples 4-6 demonstrate their  $ARF$  values within the range of  $\sim 5.4$  to  $\sim 6.1$ , implying ice adhesion strength on the low-hysteresis superhydrophobic surfaces a few times lower than on the flat fluoropolymer sample 2. Also, instead of a direct correlation between the surface  $CA$  and decreased ice adhesion strength, previously reported for both flat [14] and rough [11] surfaces, the shear stress (of ice detachment) values on rough samples 3-6 are seen to correlate with their  $CAH$  (compare the light-grey and dark-grey columns in Fig.4). This is believed to result from different ice-solid contact areas on rough surfaces, which are realized on the rough samples with different values of  $CAH$ . Such contact areas are expected to be inherited mainly from the initial water-solid contact areas during icing, and the water-solid contact area on rough surfaces with similar surface chemistry is expected to be directly related to their  $CAH$  [18]. This correlation between the ice adhesion strength on superhydrophobic surfaces and their  $CAH$  was not observed in the previous study of Saito *et al.* [11] since all their samples appeared to have low  $CAH$  values and ice was

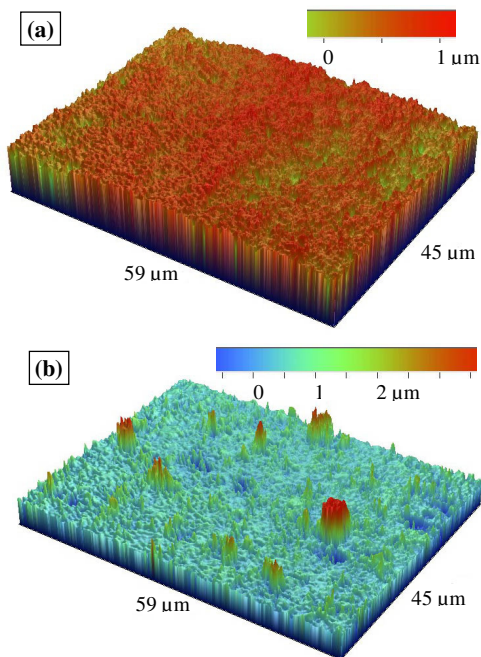


Fig. 3. Surface images of samples 3 (a) and 4 (b) taken by optical profiler.

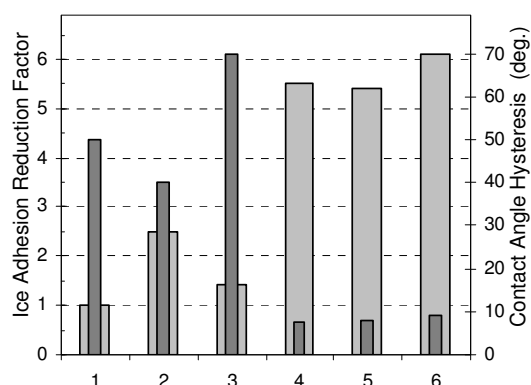


Fig. 4. Ice adhesion reduction factor (light-grey bars) and CAH (dark-gray bars) for bare polished aluminium (1); fluoro-polymer coated polished aluminium (2); superhydrophobic sample 3 with high wetting hysteresis (3); superhydrophobic samples 4 (4), 5 (5) and 6 (6) with low wetting hysteresis.

prepared by simply freezing water on top of the samples. Under such conditions, the ice-solid contact area is expected to decrease with increase in CA. This explains quite well why the Teflon-based samples in [11] demonstrated ice repellency improving with increased CA values, which is also the case for the low-CAH superhydrophobic samples observed in this study. As in the present work we tested samples with contrasting CAH, the effect of CAH on the ice adhesion strength of rough superhydrophobic surfaces was found. It should be also mentioned that ice accumulation on the high-CAH sample took significantly shorter time than on its low-CAH counterparts. Therefore, it is only the low-CAH superhydrophobic surfaces that can be considered truly ice-repellent.

#### IV. CONCLUSIONS

The adhesion of ice, prepared from super-cooled water droplets and thus similar to that accreted on outdoor structures, was measured on hydrophobic and superhydrophobic coatings with similar chemical composition, and compared to that on uncoated polished aluminium. On the superhydrophobic surfaces observed in this study, ice adhesion correlates rather with wetting hysteresis of the surfaces, being lower on low-hysteresis surfaces. This can be explained by the larger water-solid (and thus ice-solid) contact area that is expected for the high-hysteresis sample. On superhydrophobic surfaces with low wetting hysteresis, ice adhesion strength was observed to be up to about six times lower than that on bare polished aluminium.

#### V. ACKNOWLEDGMENTS

This work was carried out within the framework of the NSERC/Hydro-Quebec/ UQAC Industrial Chair on Atmospheric Icing of Power Network Equipment (CIGELE) and the Canada Research Chair on Engineering of Power Network Atmospheric Icing (INGIVRE) at Université du Québec à Chicoutimi. The authors would like to thank the

CIGELE partners (Hydro-Quebec, Hydro One, Réseau Transport d'Électricité (RTE) and Électricité de France (EDF), Alcan Cable, K-Line Insulators, Tyco Electronics, Dual-ADE, and FUQAC) whose financial support made this research possible.

#### VI. REFERENCES

- [1] S. Frankenstein and A.M. Tuthill, "Ice adhesion to locks and dams: past work; future directions?" *J. Cold. Reg. Eng.*, vol.16, pp.83-96, 2002.
- [2] V.K. Croutch and R.A. Hartley, "Adhesion of ice to coating and the performance of ice release coating," *J. Coat. Technol.*, vol.64, pp.41-52, 1992.
- [3] J.L. Laforte, M.A. Allaire, and J. Laflamme, "State-of-the-art on power line de-icing," *Atm. Res.*, vol.46, pp.143-158, 1998.
- [4] L.O. Andersson, C.G. Golander, and S. Persson, "Ice adhesion to rubber materials," *J. Adhes. Sci. Technol.*, vol.8, pp.117-132, 1994.
- [5] E.H. Andrews, H.A. Majid, and N.A. Lockington, "Adhesion of ice to a flexible substrate," *J. Mater. Sci.*, vol.19, pp.73-81, 1983.
- [6] S.A. Kulinich and M. Farzaneh, "Hydrophobic properties of surfaces coated with fluoroalkylsiloxane and alkylsiloxane monolayers," *Surf. Sci.*, vol.573, pp.379-390, 2004.
- [7] H. Wang, L.M. Tang, X.M. Wu, W.T. Dai, and Y.P. Qiu, "Fabrication and anti-frosting performance of super hydrophobic coating based on modified nano-sized calcium carbonate and ordinary polyacrylate," *Appl. Surf. Sci.*, vol.253, pp.8818-8824, 2007.
- [8] B. Somlo and V. Gupta, "A hydrophobic self-assembled monolayer with improved adhesion to aluminum for deicing application," *Mech. Mater.*, vol.33, pp.471-480, 2001.
- [9] R. Menini and M. Farzaneh, "Elaboration of Al<sub>2</sub>O<sub>3</sub>/PTFE icephobic coatings for protecting aluminium surfaces," *Surf. Coat. Technol.*, vol.203, pp.1941-1946, 2009.
- [10] C. Laforte and A. Beisswenger, "Icephobic material centrifuge adhesion test," *Proc. IWAIS XI*, pp.357-360, 2005.
- [11] H. Saito, K. Takai, and G. Yamauchi, "Water- and ice-repellent coatings," *Surf. Coat. Int.*, vol.80, pp.168-172, 1997.
- [12] S.A. Kulinich and M. Farzaneh, "On wetting behavior of fluorocarbon coatings with various chemical and roughness characteristics," *Vacuum*, vol.79, pp.255-264, 2005.
- [13] T. Kako, A. Nakajima, H. Irie, Z. Kato, K. Uematsu, T. Watanabe, and K. Hashimoto, "Adhesion and sliding of wet snow on a super-hydrophobic surface with hydrophilic channels," *J. Mater. Sci.*, vol.39, pp.547-555, 2004.
- [14] V.F. Petrenko and S. Peng, "Reduction of ice adhesion to metal by using self-assembling monolayers (SAMs)," *Can. J. Phys.*, vol.81, pp.387-393, 2003.
- [15] M. Landy and A. Freiburger, "Studies of ice adhesion. I. Adhesion of ice to plastics," *J. Colloid Interface Sci.*, vol.25, pp.231-244, 1967.
- [16] H.H.G. Jellinek, "Ice adhesion," *Can. J. Phys.*, vol.40, pp.1294-1309, 1962.
- [17] H.I. Hsiang, M.T. Liang, H.C. Huang, and F.S. Yen, "Preparation of superhydrophobic boehmite and anatase nanocomposite coating films," *Mater. Res. Bull.*, vol.42, pp.420-427, 2007.
- [18] S.A. Kulinich and M. Farzaneh, "Effect of contact angle hysteresis on water droplet evaporation from super-hydrophobic surfaces," *Appl. Surf. Sci.*, vol.255, pp.4056-4060, 2009.
- [19] M. Miwa, A. Nakajima, A. Fujishima, K. Hashimoto, and T. Watanabe, "Effects of the surface roughness on sliding angles of water droplets on superhydrophobic surfaces," *Langmuir*, vol.16, pp.5754-5760, 2000.
- [20] W. Chen, A.Y. Fadeev, M.C. Hsieh, D. Öner, J. Youngblood, and T.J. McCarthy, "Ultrasuperhydrophobic and ultralyophobic surfaces: some comments and examples," *Langmuir*, vol.15, pp.3395-3399, 1999.
- [21] S. Suzuki, A. Nakajima, M. Sakai, J.-H. Song, N. Yoshida, Y. Kameshima, and K. Okada, "Sliding acceleration of water droplets on a surface coated with fluoroalkylsilane and octadecyltrimethoxysilane," *Surf. Sci.*, vol.600, pp.2214-2219, 2006.

Author address: Prof. M. Farzaneh, Chairholder, NSERC/Hydro-Québec/UQAC Industrial Chair on Atmospheric Icing of Power Network Equipment and Canada Research Chair on Engineering of Power Network Atmospheric Icing (INGIVRE), Université du Québec à Chicoutimi 555, Boulevard de l'Université, Chicoutimi, Québec, Canada, G7H 2B1, E-mail: [farzaneh@uqac.ca](mailto:farzaneh@uqac.ca)